

DEVELOPMENT OF ELECTROSEISMIC EXPERIMENTAL METHODS

Seth S. Haines, Geophysics Department, Stanford University, Stanford, CA

Steven R. Pride, Lawrence Berkeley National Laboratory, Berkeley, CA

Simon L. Klemperer, Geophysics Department, Stanford University, Stanford, CA

Biondo L. Biondi, Stanford Exploration Project, Stanford University, Stanford, CA

ABSTRACT

The electroseismic method offers the possibility of imaging thin (much smaller than the seismic wavelength) layers and providing other valuable subsurface information. The development of experimental methods in electroseismics is essential before the method can be reliably used in shallow geophysical surveys. We have conducted experiments at two test sites and have acquired a large volume of electroseismic data, testing various data-collection geometries and methodologies. Our primary site consists of two parallel sand-filled trenches two meters apart which we image with horizontally traveling waves. Our second site is a small clearing in a culturally quiet redwood forest, where we can collect data with a minimum of background electrical noise. Our field data show the two forms of documented electroseismic phenomena, including interface-response energy from the trenches at the first site. Experiments at both sites also demonstrate the existence of a previously undocumented electroseismic phenomenon, an electric field created by a bipolar (impact) seismic source, analogous to the seismic direct wave. These experiments illustrate the effectiveness of the electroseismic method in the detection of thin layers, provide an important step toward the development of electroseismic experimental methods, and provide data on which to test signal/noise separation algorithms.

INTRODUCTION

Shallow geophysical surveys are limited in their ability to image thin layers, and to adequately characterize permeability variation. Electrokinetic phenomena represent the inter-relation between mechanical energy, fluid flow, and electrical energy. Two distinct types of electroseismic phenomena have been observed in the field, beginning with the initial experiments conducted by Thompson (1936) and continuing with experiments by Thompson and Gist (1993), Butler et al. (1996), Garambois and Dietrich (2001), and Haines et al. (2003). Development of the relevant electroseismic theory by Pride (1994), Pride and Haartsen (1996), and Haartsen and Pride (1997) affords us a clear understanding of the physics behind the observed phenomena and suggests that the electroseismic method could provide useful new information about thin layers and flow properties.

A compressional wave traveling through a fluid-saturated porous material carries with it a charge separation created by the pressure-induced flow of pore fluid. The pore fluid carries a small (but consequential) amount of electric charge relative to the adjacent grains due to the electric double layer (Shaw, 1992) that exists at the grain-fluid boundary (**Figure 1**). The strength and polarity of the electric double layer varies with grain composition and fluid chemistry, but often (such as for quartz grains) the grain surface charge is negative and the fluid positive. The net flow of charge relative to the grains is a streaming current that creates a charge separation within the seismic wave. This charge separation creates an electric field which we refer to as the “coseismic” field that is co-located with a compressional (P) wave (Pride, 1994) (**Figure 2a**). This is the most commonly and most easily observed electroseismic phenomenon. It differs from the horizontal component of

ground acceleration only in phase and amplitude because of the close relation between grain/fluid acceleration and the coseismic field.

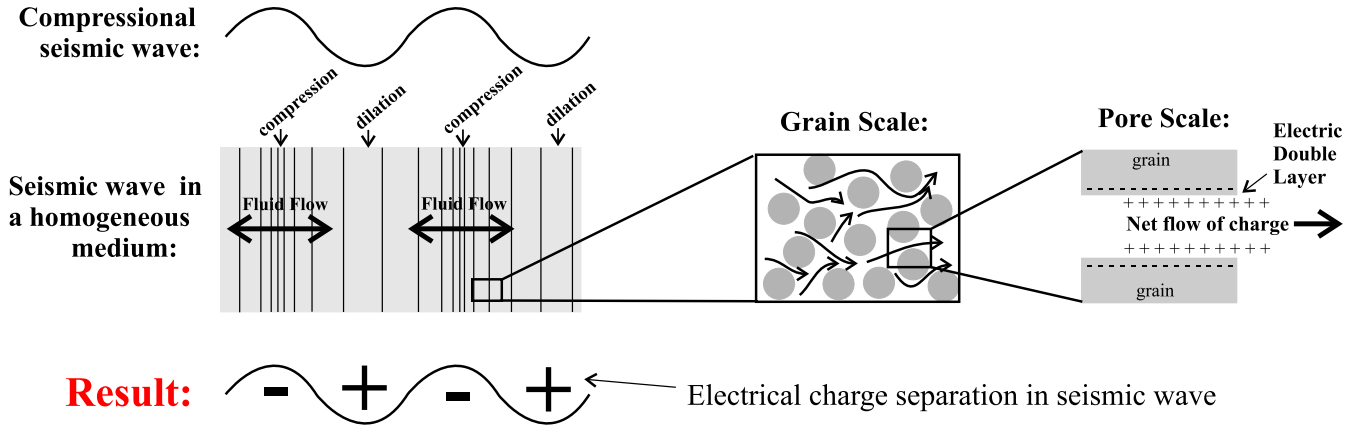


Figure 1: Electro seismic phenomena depend on the charge separation created by streaming currents that flow in response to the pressure gradient of a seismic wave. The electric double layer is responsible for streaming currents at the grain scale.

The second recognized electro seismic phenomenon occurs when the P-wave encounters an interface in material properties (elastic, chemical, flow-related, etc). The charge separation in the wave is disturbed (**Figure 2b**), causing asymmetry, and resulting in what can be approximated as an oscillating electric dipole with its dominant contribution coming from the first seismic Fresnel zone (Thompson and Gist, 1993; Haartsen and Pride, 1997). Essentially, the entire region of the first Fresnel zone acts as a disk of vertical electric dipoles. Thus, the resulting electric potential distribution is that of a dipole:

$$V(x, z) = \frac{qd}{4\pi\epsilon} \frac{z}{(x^2 + z^2)^{3/2}}, \quad (1)$$

where x is the lateral offset, z is the depth to the interface, ϵ is the electrical permittivity, and q is the magnitude of the charges that are separated by distance d . This field (**Figure 2b**), called the “interface response,” can be measured almost immediately at the Earth’s surface since the travel-time of electromagnetic radiation is negligible compared with that of seismic waves ($V_{EM} \approx 10^5 V_P$). Unlike the coseismic field, which contains information only about the immediately surrounding material, the interface response can provide useful new subsurface information. In particular, the interface response occurs even for very thin layers, such as thin fractures in otherwise solid rock, or a thin impermeable layer in an aquifer or reservoir.

A third type of electro seismic phenomenon is predicted by Equation 144 of Pride and Haartsen (1996), but observations have not yet been reported in the literature. We term this the “direct field”, as it can be thought of as analogous to the seismic direct wave. A bipolar seismic source (e.g. a sledgehammer, as opposed to a monopolar source such as a buried explosion) creates an asymmetric pressure wave. The pressure wave causes the flow of charge (via the electrokinetic effects described above) but the charge on one side of the source (in the earth, for the hammer example) is not balanced by any opposite charge on the other side (above the earth’s surface, for the hammer example), resulting in an asymmetric charge distribution. This charge distribution amounts to an oscillating electric dipole at the source point (**Figure 3**) and its field is measured directly by the electrode array. Similar to the interface response, the direct field shows the amplitude pattern

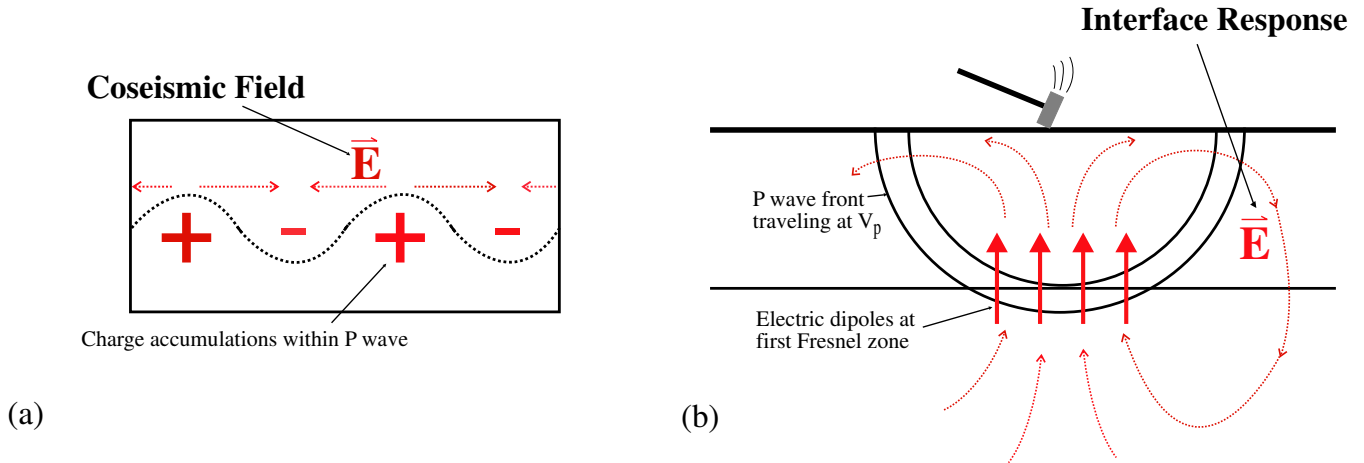
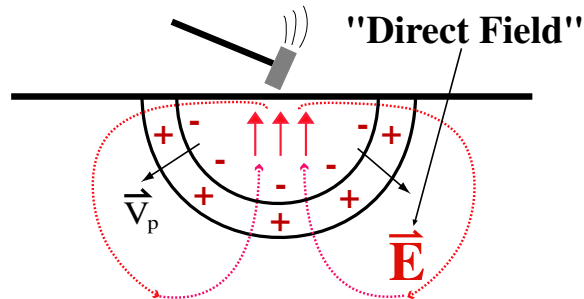


Figure 2: Two types of electroseismic phenomena commonly measured in the field: (a) the coseismic field of a P-wave (due to the charge accumulations “+” and “-”), and (b) the interface response created when the P-wave hits an interface at depth.

of a dipole (equation 1) and reversed polarity on opposite sides of the shot point. It occurs at the time of the source impulse, and continues until the earth has relaxed to its original state.

Figure 3: Schematic representation of the electroseismic direct field. The pressure wave from the source creates an asymmetrical charge distribution that acts as an oscillating electric dipole whose field is measured directly by the surrounding electrodes.



The electroseismic method promises to provide valuable information about important subsurface targets that can not be imaged using other geophysical methods, including information about changes in flow properties. However, electroseismic data (when collected with a geometry similar to conventional surface seismic data) is comprised of the interface response from subsurface layers and unwanted coseismic and direct field energy recorded simultaneously (**Figure 4a**). The direct field occurs only for a brief period after time zero so does not present a problem in surveys targeting layers deeper than a few meters. Coseismic energy, often orders of magnitude stronger than the interface response, represents a formidable form of coherent source-generated noise that can obscure large parts of the electroseismic record. We employ specifically-developed experimental designs that allow us to record all three electroseismic phenomena separately. These data provide an ideal data set for testing data processing algorithms along with providing greater insight into the electroseismic phenomena themselves.

We begin by describing our experimental designs, then outline our field methods and discuss data examples. We present the first published observations of the electroseismic direct field.

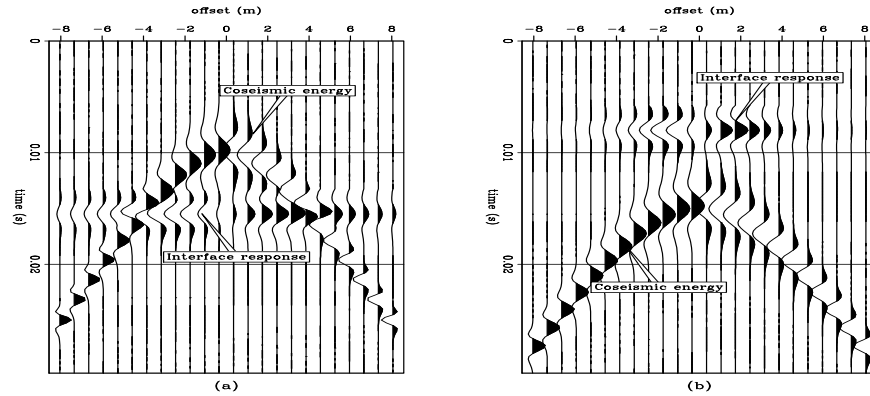


Figure 4: Generalized electroseismic data for two different recording geometries. For simplicity we assume a monopolar source, and so neglect the direct field. Amplitude pattern of interface response is modeled using Equation (1). Amplitudes of coseismic arrivals are constant for simplicity; we do NOT account for attenuation or spherical divergence. (a) Data recorded with a “in-line” geometry, as shown in **Figures 2b** and **9**, show coseismic energy and interface response recorded simultaneously. (b) Data recorded with source and receivers on opposite sides of a vertical interface (“fan” geometry, as shown in **Figure 9**) show the interface response arriving before the coseismic energy.

EXPERIMENTAL METHODS

Data collection

Following Haines et al. (2001), we collect electroseismic data using a standard engineering seismograph, in our case a Geometrics 24-channel Geode, sometimes augmented with a second 24-channel Geode. The geophone cables are outfitted with electrode pairs rather than geophones. Thus each channel of the seismograph records the voltage difference across a given pair of electrodes. Our electrodes are 3/8 inch steel rods that are ~ 0.7 m long with sharpened tips, pounded almost completely into the ground. We typically use a spacing of ~ 1 m between the two electrodes in a given pair, and overlap electrode pairs if necessary to achieve station spacing smaller than dipole width. In order to eliminate the resonant electrical noise caused by the lightning protection circuitry in the seismograph, we insulate each channel of the instrument from the electrodes with a 5:1 step-up transformer (Art Thompson, personal communication September 2001). When the ground is dry, we improve electrode coupling by wetting each electrode hole thoroughly with water. We find that the addition of conductive agents such as salts or bentonite clay offers only minimal improvement over tap water for our generally clay-rich field areas.

We have tested various seismic sources including shotgun and an electromagnetic vibrational source, but achieve the most consistent results by stacking 10 to 50 sledgehammer strikes. Because of the time-variable nature of electrical noise we perform the final stack in the office, after manually removing individual noisy shots. We have tested various hammer plates, including plastic and different metals, to determine strike-to-strike repeatability and to identify any associated electrical noise related to the hammer plate.

All of the data presented in this paper are electroseismic data collected using one of two different recording geometries:

- “*in-line*” geometry: Source location is in the center of electrode receiver array, similar to a standard split-spread seismic deployment.
- “*fan*” geometry: Source location a distance away from the center of the receiver array, in a direction perpendicular to the array. Similar to a seismic fan deployment.

We generally record one-second records at a sample rate of 4000 Hz, including a half-second of pre-trigger recording for noise estimation. Typical signal measurements are on the order of 0.1 mV for the coseismic energy, and 0.001 mV for the interface response in stacked records. Noise levels are typically ~ 0.01 mV for 60 Hz noise, and ~ 0.001 mV for background electrical noise at our vineyard field site. At the treefarm site we find 60 Hz noise levels of ~ 0.001 mV and background electrical noise at ~ 0.0002 mV for stacked records.

Field Site I: Pride Vineyard

By placing source and receivers on opposite sides of a vertical interface it is possible to record the interface response before the coseismic energy because the seismic wave encounters the interface and creates the interface response before the seismic wave (and associated coseismic field) reaches the receiver electrodes (**Figure 4b**). In order to achieve this geometry, we constructed a trench ~ 0.6 m wide, ~ 2 m deep, and ~ 18 m long, lined with plastic, and filled with wet sand, at a site with relatively homogeneous clayey soil to at least 5m depth (**Figures 5 and 6**). The site is a small meadow at the Pride Mountain Vineyards on the ridge between Napa and Sonoma Valleys in St. Helena, CA.

Figure 5: Site construction. The first trench is 18 meters long, two meters deep, and about 0.6 m wide. It is dug in relatively homogeneous clayey soil.



After successfully observing the interface response with the one-trench geometry (**Figures 7 and 8**), we constructed a second trench (**Figure 9**) approximately two meters from the first, in order to increase the experiment complexity. It is deeper (~ 3 m deep in the center), narrower (~ 0.5 m wide), and lacks the plastic sheeting that lines the first trench.

The geometry of this field site provides a great deal of versatility in recording geometry. We can place sources and receivers on opposite sides of the trenches in order to record the interface response before the coseismic energy, simulating a cross-well type geometry (“Fan-geometry source point”, in **Figure 9**). To simulate a “typical” surface survey of subsurface targets (the geometry generally used in surface seismic, and shown in **Figure 2b**) we have also collected data with the source located on the same side of the trench as the receivers (“In-line source point”, in **Figure 9**). In this case the coseismic energy and interface response are recorded simultaneously. In addition, we conducted a survey in the same meadow, but ~ 20 m from the trenches, as a control study, also using the “in-line” geometry.

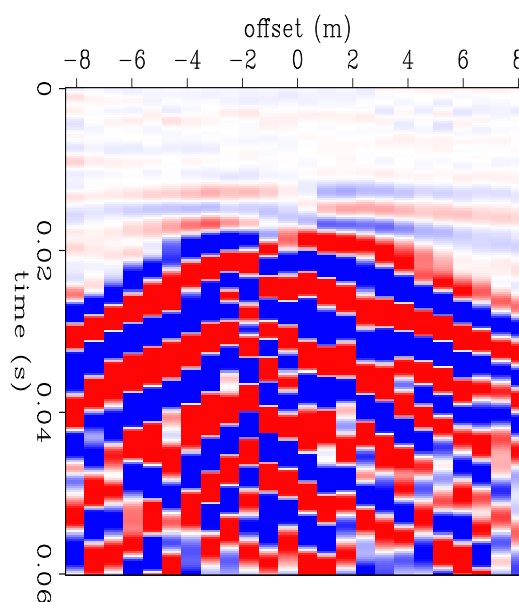
Figure 6: The first trench was lined with plastic and filled with sand and water. The second trench was not lined with plastic.



Figure 7: Data acquisition prior to construction of second trench, using “fan” geometry. Source point in this photo is one meter from one side of the trench, and receiver line is one meter from the opposite side of the trench. Shooter is standing in the trench, with PVC piezometers on either side of him that are used to measure water table in trench.



Figure 8: “Fan” geometry shot record recorded with source and receivers two meters from opposite sides of the first trench (before construction of the second trench). Record is the result of stacking 50 hammer strikes and is shown with 60 Hz energy removed and bandpass filter (120-500 Hz) applied. Note horizontal interface response event at 0.015 seconds.



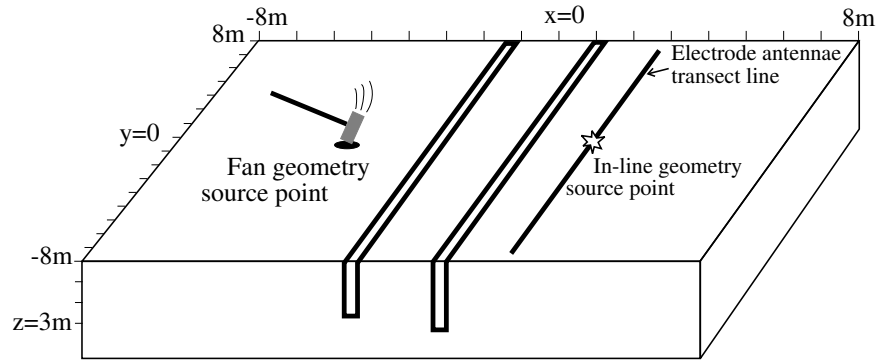


Figure 9: Layout of vineyard field site after construction of second trench. Electro seismic data was acquired with both recording geometries, as shown.

Site II: Thompson Tree Farm

We also conduct experiments at the Thompson redwood tree farm in the Santa Cruz Mountains on the San Francisco peninsula. This site is far removed from cultural noise, including the power grid, so is ideal for collecting quiet electrical data. The site itself is a small level clearing with clayey soil. Seismic and geologic data suggest that bedrock is a few meters deep, and that the soil/bedrock contact is rather diffuse.

We use this site to test basic field methodologies and have not recorded, and do not expect to record, strong interface response energy. We have collected data with 0.7m spacing between channels and various dipole widths. Using the “in-line” geometry we conducted a series of experiments with different types of impact source in order to better understand the effects of source composition (e.g. wood, plastic, and metal) as well as the triggering circuitry.

Data pre-processing

Raw electroseismic data is dominated by energy from the power grid at harmonics of 60 Hz. We remove this noise using the sinusoid subtraction technique of Butler and Russell (1993) for all harmonics of 60 Hz up to the Nyquist frequency. Coseismic energy is generally lower in frequency than the interface response due to a greater distance of travel as a seismic wave, so we use a low-cut filter to begin the process of noise removal. (Because the electromagnetic wavelength associated with the interface response is tens of kilometers, attenuation of the electromagnetic energy is negligible.) We employ a high-cut filter to minimize background noise that can obscure weaker arrivals. **Figure 8** shows a typical shot gather after these processing steps. We do not find any evidence of data contamination by AM radio broadcasts, a problem encountered using similar instrumentation at other sites (Karl Butler, personal communication, 2003). This problem is likely site-dependent, and seems not to be present at our sites.

FIELD DATA

Data review- observing the direct field

We begin by considering a simple electroseismic shot gather (**Figure 8**) from the vineyard site. With the shot and receivers on opposite sides of a single trench (“fan” geometry) we expect to see an interface response event followed by the arrival of coseismic energy. We do observe this pattern, with the flat interface response energy at ~ 15 ms, and curved coseismic energy dominating the later part of the record. A similar geometry,

but with two trenches between the source and receivers is shown in **Figure 10a** and shows roughly what we expect- the interface response energy from the second trench (the trench nearer the receivers) is clearly visible at ~ 18 ms, followed by coseismic energy. We would expect to see the interface response arrival from the first trench at ~ 7 ms, but find that it is either very weak or absent due to the distance from the interface to the receivers and the r^2 amplitude fall-off of the potential field of a dipole.

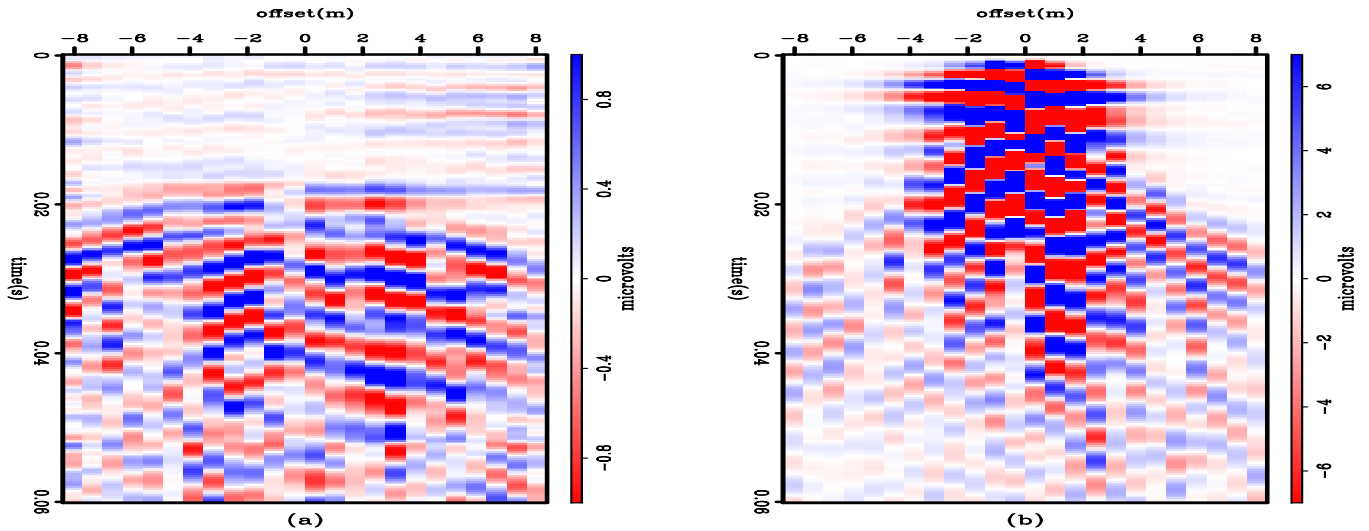


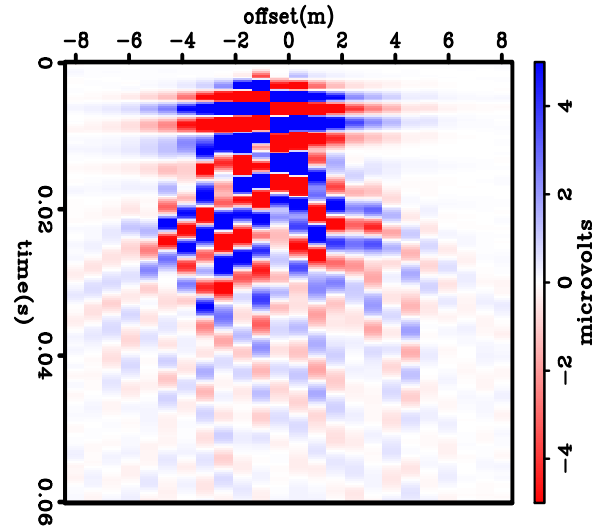
Figure 10: Two 24-channel shot gathers recorded simultaneously at the vineyard site using 25 hammer strikes located ~ 1.5 m from the edge of the first trench. a) “Fan” geometry. Electrode receivers are located 1.5m from the edge of the second trench (opposite the shot location). Interface response from the second trench is clearly visible at ~ 18 ms, followed by curved coseismic energy. b) “In-line” geometry. Electrode receivers located in line with the shot position, 1.5 m from the first trench. Dipping coseismic energy is present, along with flat events whose interpretation is discussed in the text.

We next consider the more complex case of the source and receivers in a single line on one side of the two trenches (“in-line” geometry). For this case we expect to see interface response events corresponding with the two trenches, simultaneous with coseismic energy. Such data collected at the same time (same source, two receiver lines) as that in **Figure 10a** is shown in **Figure 10b**. These data appear to show exactly this pattern- several flat events in the upper 20ms of the record, along with the curved coseismic energy. Closer inspection, however, exposes a problem with this interpretation. The first flat event in the record appears to begin practically at time zero, rather than at the delay which would be expected for the compressional wave to reach the first trench. This suggests that the signal at time zero is related to the source, rather than to the incidence of the compressional wave on the trench.

We investigate the discrepancy between the expected and observed results by considering control data collected in the same meadow as the trenches (and with what we assume to be comparable geology), but ~ 20 m away from the trenches. In these “in-line” geometry data, we expect to see coseismic energy, but no flat interface response events. The data (**Figure 11**), however, show a pattern very similar to that of **Figures 10b**, with flat events in the upper ~ 15 ms and coseismic energy throughout. So we must conclude either that the flat events are not interface response energy, or that they are interface response events from some very shallow layer. From geologic and geophysical observations we are confident that no sharp interfaces exist in the upper few meters at this site. From testing various hammer plate options (plastic and various metals) we are confident that this signal is not related to the electromagnetic effects of the movement of metal hammer

plates.

Figure 11: 24 channel electroseismic record collected at the vineyard site, away from the trenches with 25 hammer strikes. Source is in center of electrode array (“in-line” geometry). Clearly visible are flat events in the upper ~ 15 ms, and dipping coseismic energy.



In order to better understand this source-related dipole, and to determine whether it is the electroseismic direct field, we consider the data collected at the tree farm site (**Figure 12**). We examine a series of four shot gathers collected with the source point in the center of a line of 0.7m-spaced electrode receivers (“in-line” geometry). The first, and simplest, experiment is to simply trigger the seismograph without actually putting any seismic energy in the ground. We strike the hammer trigger switch against a solid object, stack 25 records (as for the hammer stacks), and find only background electrical noise in the record (**Figure 12a**), demonstrating that the trigger mechanism is not responsible for the observed signal. Next we use a manual wooden weight-drop source (a 4 inch x 4 inch fence post) on a plastic plate, and collect the data shown in **Figure 12b**. These data show the flat source-related energy in the upper ~ 15 ms, along with the dipping coseismic energy. For comparison, we also show (**Figure 12c**) a similar-looking record resulting from stacking 25 hammer strikes on the plastic plate, demonstrating that motion of the metal hammer head is not responsible for the observed signal. Thus we conclude that this energy must be the direct field predicted by Pride and Haartsen (1996). A final experiment, with the fence post on a cylindrical aluminum hammer plate (**Figure 12d**), shows direct field energy as in the previous records, but also another form of source-related energy. We observe a flat arrival with amplitudes similar to those of a dipole, but with the same polarity on the both sides of the shot point. We infer that this energy is the electric field resulting from moving the conductive hammer plate in the earth’s magnetic field. This interpretation is consistent with the fact that this energy varies greatly between individual hammer strikes, along with the magnitude of motion of the hammer plate. This field is not observed in data collected under dry conditions at the vineyard site, and also is not observed at the tree farm site when the aluminum plate is insulated from the earth by a layer of cloth.

As a summary, **Figure 13** features our interpretation of a 48 channel, “in-line” geometry, shot record similar to the 24-channel record shown in **Figure 10b**. The flat arrivals in the upper ~ 15 ms are the direct field, followed by a weak interface response arrival at ~ 20 ms. The remaining energy, mostly higher amplitude and curved/dipping, is the coseismic energy.

Quantifying the measured signal

Further certainty in our interpretations can be gleaned from simple amplitude modeling of the observed signals. Using Equation (1) we predict the amplitude pattern for our acquisition geometries. Because of the difficulty of determining appropriate values for the constants in Equation (1), we set the distance terms (x and z) and then scale the result to match the absolute amplitudes that we observe. **Figure 14a** shows a comparison

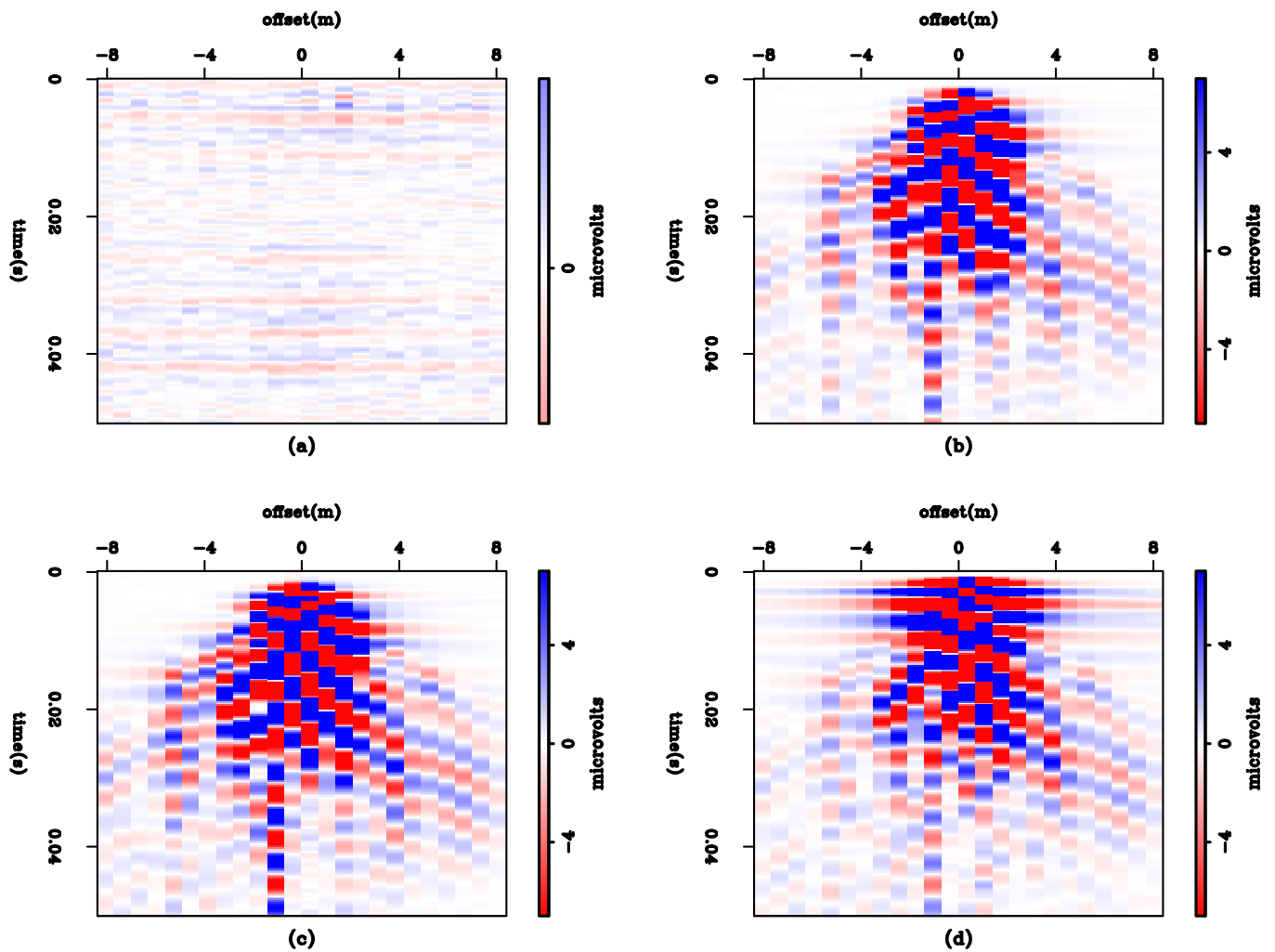
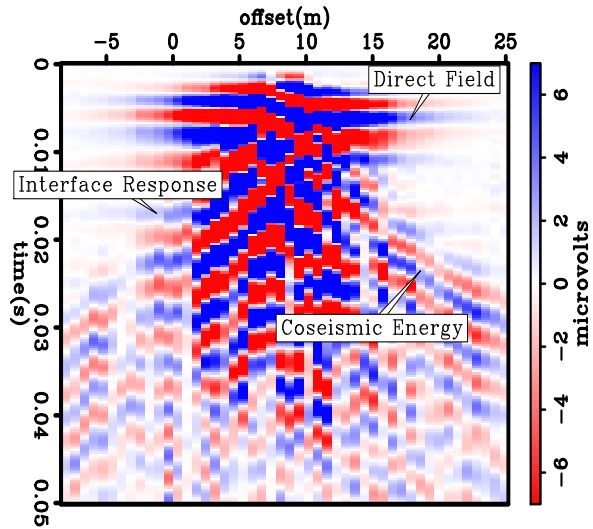


Figure 12: Shot gathers from the tree farm site. a) stack of data collected by striking the trigger switch against a solid object not in contact with the ground. b) stack of 25 strikes of a wooden post on a plastic plate, showing flat events in the upper ~ 18 ms and dipping coseismic energy. c) stack of 25 strikes of a sledgehammer on a plastic plate; appearance is very similar to b). d) stack of 25 strikes of sledgehammer on cylindrical aluminum hammer “plate”, showing additional source-related flat event with same polarity on both sides of shot point.

Figure 13: 48 channel “in-line” geometry electroseismic shot gather from the vineyard site, annotated with our interpretations identifying the three different electroseismic phenomena.



between the actual amplitudes for the interface response event in **Figure 10a** (dots) and the amplitude pattern predicted by Equation (1) (solid line). The two compare reasonably well given the signal/noise ratio present in the data, supporting our interpretations. **Figure 14b** shows the amplitudes for the first phase of the direct field of the data in **Figure 12b** (dots) and the predicted amplitudes (solid line) based on a dipole depth of 0.25 m, which is consistent with our understanding of the direct field.

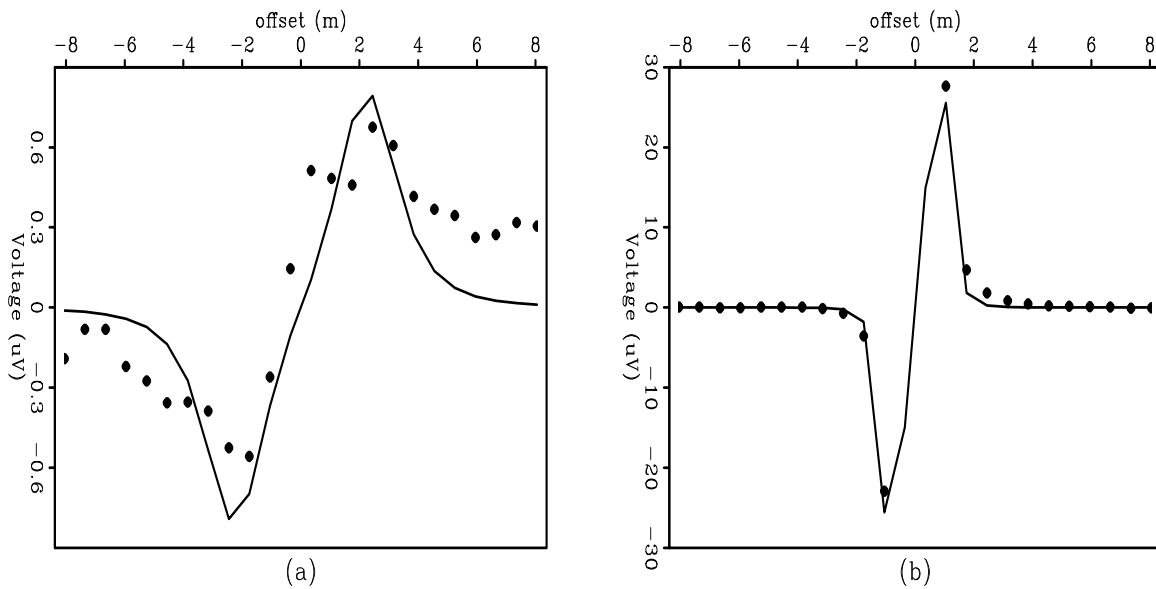


Figure 14: Comparison between actual (dots) and predicted (solid lines) amplitudes for a) the interface response event in **Figure 10a** and b) the direct field event in **Figure 12b**. The predicted amplitude pattern for the direct field is based on a depth of 0.25 m to the dipole, and a dominant frequency of 100 Hz.

CONCLUSIONS

By horizontally imaging a vertical interface we can separate the electroseismic interface response from the coseismic energy, allowing us to better study the two forms of energy. We also present the first reported observations of the electroseismic direct field. This finding is valuable in terms of advancing our understanding of electroseismic phenomena, and also in terms of possible applications of the direct field to geophysical problems.

We have also established that the use of a metal sledgehammer source does not create electrical noise, but that the use of a metal hammer plate may cause electrical noise if it is sufficient electrical contact with the ground (if the plate is uninsulated from wet soil).

Although not yet at a stage where it can be applied to geophysical problems of interest, the electroseismic method promises to provide useful new information about the subsurface, including information about thin layers and flow property variations. Our work represents important progress toward that goal.

ACKNOWLEDGMENTS

The data presented here would not exist without the effort of those who swung the hammer: Nick Martin, Jordan Muller, Brian Ebel, Mike Beman, Phil Resor, T.J. Kiczenski, Stephan Bergbauer, Antoine Guitton, Morgan Brown, and Jonathan Franklin. Jerry Harris has been an important source of insight and guidance since the inception of this project. Jim and Carolyn Pride graciously provided the field site, ten dump trucks full of sand, and some of their outstanding wine. Art Thompson provided some essential electronics, along with important input on data collection. Data processing has largely been accomplished on the Stanford Exploration Project (SEP) computer system, with much help from SEP students including Antoine Guitton, Morgan Brown, Bob Clapp, Brad Artman and Marie Clapp. Funding has been provided by the Petroleum Research Fund, the Achievement Rewards for College Scientists Foundation, the Stanford School of Earth Sciences McGee Fund, the AAPG student research grants program, the GSA student research grants program, the Colorado Geological Survey and the Stanford Exploration Project.

REFERENCES

- Butler, K. E., and Russell, R. D., 1993, Subtraction of powerline harmonics from geophysical records (short note): *Geophysics*, **58**, no. 06, 898–903.
- Butler, K. E., Russell, R. D., Kepic, A. W., and Maxwell, M., 1996, Measurement of the seismoelectric response from a shallow boundary: *Geophysics*, **61**, no. 06, 1769–1778.
- Garambois, S., and Dietrich, M., 2001, Seismoelectric wave conversions in porous media: Field measurements and transfer function analysis: *Geophysics*, **66**, no. 5, 1417–1430.
- Haartsen, M. W., and Pride, S. R., 1997, Electroseismic waves from point sources in layered media: *J. Geophys. Res.*, **102**, no. B11, 24745–24769.
- Haines, S., Pride, S., and Klemperer, S., 2001, Development of experimental methods in electroseismic research, with application to aquifer characterization: *Eos Trans. AGU*, **82**, no. 47, Abstract GP22A–0268.

- Haines, S., Guitton, A., Biondi, B., and Pride, S., 2003, Development of experimental methods in electroseis-
mics: 73rd Ann. Internat. Mtg., Soc. of Expl. Geophys., Expanded Abstracts.
- Pride, S. R., and Haartsen, M. W., 1996, Electrostatic wave properties: *J. Acoust. Soc. Am.*, **100**, no. 3,
1301–1315.
- Pride, S., 1994, Governing equations for the coupled electromagnetics and acoustics of porous media: *Physi-
cal Review B*, **50**, no. 21, 15678–15696.
- Shaw, D., 1992, *Introduction to colloid and surface chemistry*: Butterworths, 4th edition.
- Thompson, A. H., and Gist, G. A., 1993, Geophysical applications of electrokinetic conversion: *The Leading
Edge*, **12**, no. 12, 1169–1173.
- Thompson, R. R., 1936, The seismic electric effect: *Geophysics*, **01**, no. 03, 327–335.